ChemPubSoc Europe

DOI: 10.1002/chem.201503980

CHEMISTRY
A European Journal
Full Paper

Transition Metals |*Hot Paper*|

Homoleptic Two-Coordinate Silylamido Complexes of Chromium(I), Manganese(I), and Cobalt(I)

C. Gunnar Werncke,[a] Elizaveta Suturina,[b] Philip C. Bunting,[c] Laure Vendier,[a] Jeffrey R. Long,[c] Mihail Atanasov,[b, d] Frank Neese,*[b] Sylviane Sabo-Etienne,[a] and Sébastien Bontemps*[a]

Abstract: Anionic two-coordinate complexes of first-row transition-metal(I) centres are rare molecules that are expected to reveal new magnetic properties and reactivity. Recently, we demonstrated that a $N(SiMe_3)_2^-$ ligand set, which is unable to prevent dimerisation or extraneous ligand coordination at the +2 oxidation state of iron, was nonetheless able to stabilise anionic two-coordinate Fe^I complexes even in the presence of a Lewis base. We now report analogous Cr^I and Co^I complexes with exclusively this amido ligand and the isolation of a $[Mn^I\{N(SiMe_3)_2\}_2]_2^{2-}$ dimer that features a Mn–Mn bond. Additionally, by increasing the steric hindrance of the ligand set, the two-coordinate complex $[Mn^I\{N(Dipp)(SiMe_3)\}_2]^-$ was isolated (Dipp = 2,6-*i*Pr_2-C_6H_3). Characterisation of these compounds by using X-ray crystallography, NMR spectroscopy, and magnetic susceptibility measurements is provided along with ligand-field analysis based on CASSCF/NEVPT2 ab initio calculations.

Introduction

Two-coordinate 3d metal complexes present an attractive class of compounds for applications in catalysis and materials science.[1] Sterically hindered ligands have been used to stabilise two-coordinate M^{II} and M^I complexes, with the latter being a promising new field.[2–4] The silylamido group $N(SiMe_3)_2^-$ is an ubiquitous ligand for transition metals[1b] (except for late 4d and 5d metals), lanthanides[5] and alkali metals.[6] It is remarkable that the $[M\{N(SiMe_3)_2\}_2]$ series is known as dimers or solvent adducts for M = Cr, Mn, Fe, Co at the +2 oxidation state, whereas the related iron(I) complex K(18-crown-6)$[Fe^IN(SiMe_3)_2)_2]$ (**1**) proved to be two-coordinate, as we recently published.[7] This perfectly linear complex, obtained in very high yield by the reduction of a neutral trigonal iron(II) complex (Scheme 1), does not react with Lewis bases. This result indicates that different coordination rules can be at play for the +1 oxidation state. We now report our findings concerning the synthesis of other first-row transition-metal(I) complexes. In particular, physical and quantum chemical studies provide a detailed description for the Cr, Mn, Fe, Co members of the series.

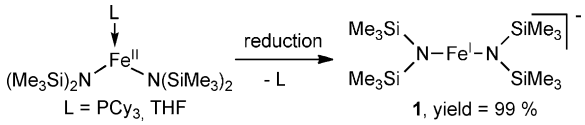

Scheme 1. Synthesis of K(18-crown-6)$[Fe^I\{N(SiMe_3)_2\}_2]$ complex **1**.

Results and Discussion

The THF adducts of Cr^{II} and Co^{II} hexamethyldisilazides were subjected to a slight excess of KC_8 in the presence of 18-crown-6 to afford K(18-crown-6)$[Co^I\{N(SiMe_3)_2\}_2]$ (**2**) and K(18-crown-6)$[Cr^I\{N(SiMe_3)_2\}_2]$ (**3**) in 82 and 71% yield, respectively. From the crystallisation mixture of complex **3**, some darker orange crystals of complex **4** with 1.5 equivalents of cryptand per anion were obtained. The use of the more encapsulating 2.2.2-cryptand allowed for the isolation of K(crypt.2.2.2)-$[Cr^I\{N(SiMe_3)_2\}_2]$ (**5**) in 78% yield (see Scheme 2).

X-ray diffraction analyses of **2** (Figure 1) and **3** (Figure S25 in the Supporting Information) revealed structures analogous to the one previously observed for **1**.[7] The metal centres lie on a crystallographic inversion centre and the $N(SiMe_3)_2^-$ ligands are in an eclipsed conformation, with the Si-N-Si planes slightly

[a] *Dr. C. G. Werncke, Dr. L. Vendier, Dr. S. Sabo-Etienne, Dr. S. Bontemps*
CNRS, LCC (Laboratoire de Chimie de Coordination)
205 route de Narbonne, 31077 Toulouse (France) and Université de Toulouse, UPS, INPT 31077 Toulouse (France)
E-mail: sebastien.bontemps@lcc-toulouse.fr
Homepage: http://www.lcc-toulouse.fr/lcc/spip.php?article433

[b] *Dr. E. Suturina, Prof. Dr. M. Atanasov, Prof. Dr. F. Neese*
Max-Planck-Institute for Chemical Energy Conversion, Stiftstrasse 34–36, Mühlheim an der Ruhr, 45470 (Germany)
E-mail: mihail.atanasov@cec.mpg.de
frank.neese@cec.mpg.de

[c] *P. C. Bunting, Prof. J. R. Long*
Department of Chemistry, University of California, Berkeley
Berkeley, California 94720 (USA)

[d] *Prof. Dr. M. Atanasov*
Institute of General and Inorganic Chemistry
Bulgarian Academy of Sciences, 1113 Sofia (Bulgaria)

Supporting information for this article is available on the WWW under http://dx.doi.org/10.1002/chem.201503980.

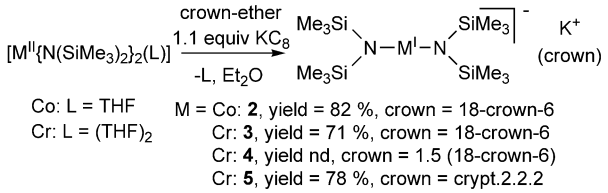

Scheme 2. Synthesis of $[M^{I}\{N(SiMe_3)_2\}_2]^-$ complexes **2**–**5** (nd = not determined).

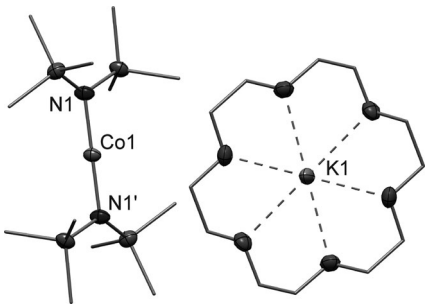

Figure 1. Molecular structure of **2**. All hydrogen atoms are omitted for clarity; thermal ellipsoids drawn at the 30% probability level.

bent with respect to the N-M-N axis ($\approx 18^\circ$ for **2** and **3**). In contrast, the X-ray analysis revealed two and three inequivalent chromium(I) anions per unit cell for **4** and **5** (Figures S26 and S27 in the Supporting Information), respectively, which show some conformational distortion compared with **1**–**3**. In the case of **5b** and **5c**, a quasi-linear N-Cr-N bond angle is observed, whereas **5a** displays a slightly more bent angle of 175.74(10)° and a more distorted conformation with somewhat twisted $N(SiMe_3)_2^-$ groups (14.42(6)°). These analyses indicate that two-coordinate structures are accessible for Co^{I} and Cr^{I} compounds with $N(SiMe_3)_2^-$ ligands. Perfectly linear geometries are found, but quasi-isoenergetic structures that deviate from linearity are also observed in the case of chromium.

When the precursor $[Mn^{II}\{N(SiMe_3)_2\}_2]$ was treated with KC_8 in the presence of 18-crown-6, a dark-violet solution was observed upon warming above −20 °C. Although in situ ^{1}H NMR spectra indicated the formation of a well-defined product (Figure S12 in the Supporting Information), the presumed manganese(I) amide proved to be highly unstable and colourless crystals of the manganese(II) compound $K(18\text{-crown-}6)[Mn^{II}\{NSiMe_3)_2\}_3]$, and also $K(18\text{-crown-}6)\{N(SiMe_3)_2\}$, were isolated (Figures S28 and S29 in the Supporting Information).[8] Faster crystallisation enabled the isolation of violet crystals, identified as a dianionic, bimetallic manganese(I) complex $[K(18\text{-crown-}6)_{1.5}]_2[Mn^{I}\{N(SiMe_3)_2\}_2]_2$ (**6**) that features an unsupported Mn–Mn bond (Scheme 3, Figure 2). Here, the Mn–N bond lengths of approximately 2.15 Å are longer by about 0.1 Å than all the other complexes (Table 1). The Mn–Mn bond length of 2.802(2) Å is comparable to those in the two other examples of tri-coordinate Mn^{I} dimers[9] and slightly longer than that of a related di-coordinate Mn^{I} dimer complex (Mn–Mn = 2.7224(6) Å).[4] The sensitivity of the complex did not enable us to further probe whether a monomeric two-coordinate Mn^{I} complex is initially formed. However, the dimerisation through a metal–metal bond formation is remarkable because it contrasts with the Mn^{II} parent compound that dimerises through bridging amide ligands.[10] It should be noted that in the case of M^{I}(1,3-diketiminate) complexes (Cr–Ni), the Mn examples were also the only ones that exhibited such a metal–metal bond.[9a,11] This feature was explained by an overlap of the 4s orbitals of the Mn^{I} ions, each of which is in a $4s^13d^5$ configuration.[9a]

To isolate a stable two-coordinate Mn^{I} amido species, we turned our attention to the more bulky $N(Dipp)(SiMe_3)^-$ (Dipp = 2,6-*i*Pr$_2$-C$_6$H$_3$) ligand set. Reaction of $MnCl_2$ with two equivalents of $Li\{N(Dipp)(SiMe_3)\}$ afforded the two-coordinate

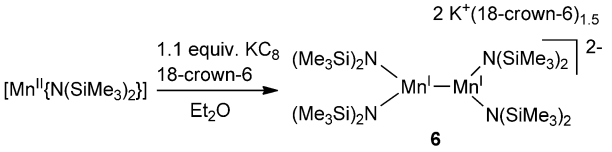

Scheme 3. Synthesis of the Mn^{I} dimer **6**.

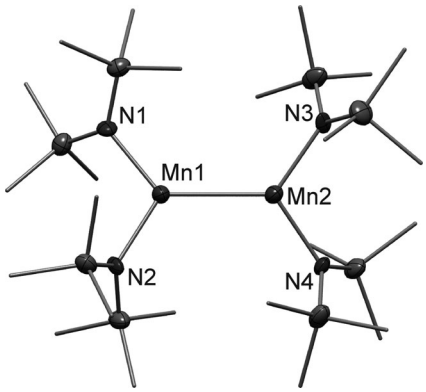

Figure 2. Molecular structure of **6**. All hydrogen atoms, K(18-crown-6) moieties, and a disorder on one $SiMe_3$ group are omitted for clarity; thermal ellipsoids drawn at the 30% probability level.

Table 1. Selected X-ray data for complexes **1**–**3**, **5**, **7**, and **8**.

	M–N [Å]	M–M[a] [Å]	M–K[a] [Å]	N-M-N [°]	Twisting angle[b] [°]
1	1.9213(6)	9.5765(2)	6.4566(2)	180	0
2	1.8979(11)	9.6542(4)	6.5128(3)	180	0
3	2.049(17)	11.1475(6)	6.5215(3)	180	0
5a	2.063(2) 2.068(2)	9.9770(8)	7.3937(8)	175.74(10)	14.42(6)
5b	2.077(3) 2.076(2)	9.9770(8)	7.4980(9)	179.48(10)	0.61(12)
5c	2.062(3) 2.061(3)	10.0617(8)	7.2709(9)	179.30(10)	13.54(6)
7	1.9182(7)	8.7868(4)	–	180	0
8	1.961(3) 1.954(3)	10.8687(11)	7.8756(12)	167.12(14)	49.1(2)

[a] Shortest distance in the crystal lattice. [b] Angle between the planes of the two amide units.

complex $[Mn^{II}\{N(Dipp)(SiMe_3)\}_2]$ (**7**) in 57% yield.[12] Reduction of **7** in the presence of 18-crown-6 afforded K(18-crown-6)$[Mn^{I}\{N(Dipp)(SiMe_3)\}_2]$ (**8**) in 60% yield (Scheme 4). Compound **8** represents a rare example of a two-coordinate Mn^{I} ion.[4,3d]

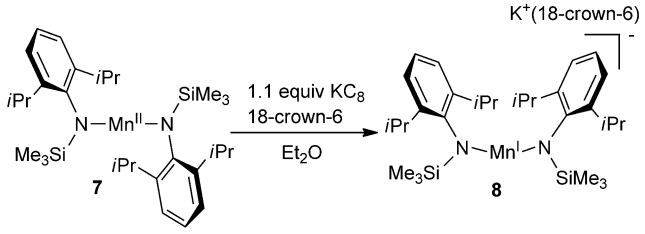

Scheme 4. Synthesis of the two-coordinate Mn^{I} complex **8** from the reduction of complex **7**.

The X-ray diffraction analysis of **7** (Figure 3A) revealed a perfectly linear structure, whereas **8** (Figure 3B) features a bent structure with a N-Mn-N angle of 167.12(14)°. The Mn–N bond lengths in **7** (1.9182(7) Å), which are the shortest so far reported for two-coordinate manganese complexes,[1b] are slightly

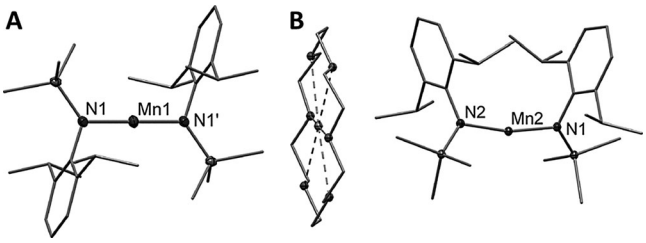

Figure 3. Molecular structure of A) **7** and B) **8**. All hydrogen atoms are omitted for clarity; thermal ellipsoids drawn at the 30% probability level.

elongated in **8** (1.954(3) and 1.961(3) Å). The orientation of the substituents on the nitrogen atom changes from *trans* in **7** to *cis* in **8**. The short separations between the manganese atom and the *ipso*-carbon atom of the phenyl ring (2.7410(7) Å in **7** and 2.799(4) Å in **8**) imply very weak secondary interactions.[1b] In addition, one isopropyl group of each ligand in **8** points towards the phenyl ring of the opposing ligand, which indicates dispersion interactions.[13]

Complexes **1**–**3**, **5** and **8** give rise to paramagnetic but well-defined NMR spectra, whereas complex **7** is NMR silent. In the variable-temperature ^{1}H NMR spectroscopy analysis of Co^{I} complex **2**, depicted in Figure 4, the chemical shift for the $SiMe_3$ groups varies from $\delta = -4.70$ ppm ($w_{1/2} = 16$ Hz) at 298 K to $\delta = -7.6$ ppm ($w_{1/2} = 125$ Hz) at 173 K. The crown-ether protons are found in the normal chemical shift range at room temperature. However, as in the case of complex **1**, upon cooling from 200 K, the signal shifts and is split into two signals of equal intensity. For Cr^{I} complexes **3** and **5**, slightly shifted signals associated with the cryptand are observed along with a large line-broadening of the crown-ether signal for **3**. For complexes **2**–

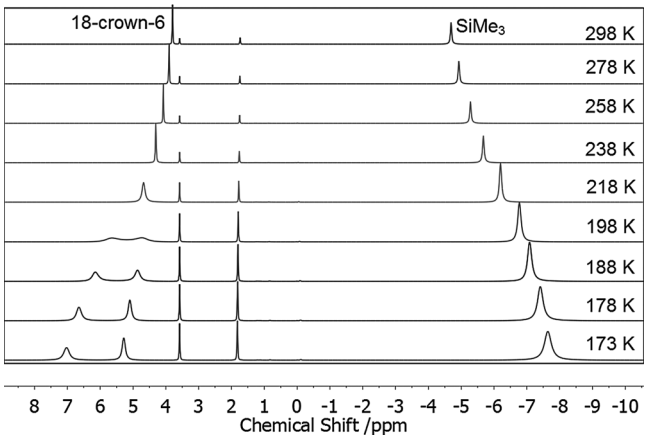

Figure 4. Variable-temperature ^{1}H NMR spectra of **2** in $[D_8]$THF.

5, both the shifts and/or the line broadening indicate an influence of the paramagnetic metal centre on the protons of the counterion, probably as a result of relatively unencumbered metal ions. The crown-ether signal for **8**, which features bulkier $N(Dipp)(SiMe_3)^-$ ligands, is indeed much less affected even upon cooling.

The solution effective magnetic moments of **3** (5.99 μ_B), **7** (6.09 μ_B) and **8** (4.98 μ_B) are close to the expected spin-only values. For complex **2**, however, the μ_{eff} value of 4.18 μ_B is higher than the value expected for a high-spin d^8 system ($\mu_{S.O.} = 2.83$ μ_B), which indicates a contribution of orbital angular momentum to the spin, as observed for iron(I) analogue **1**. Variable-temperature dc magnetic susceptibility measurements in the solid state were conducted for **2** and **8**, for which magnetic anisotropy was expected. The $\chi_M T$ values of 2.22 and 3.32 $cm^3 K mol^{-1}$ (which correspond to 4.21 and 5.15 μ_B) at room temperature for **2** and **8**, respectively, are in good agreement with the Evans' measurements. Compound **2** exhibits a steady decrease in susceptibility upon lowering the temperature, which indicates magnetic anisotropy and temperature-independent paramagnetism (Figure 5). A small field dependence at high temperature was observed, likely due to the presence of a superparamagnetic impurity. This is similar, though less pronounced, to observations already made for **1**.

For complex **8**, the $\chi_M T$ values at 0.1 and 1 T remain constant until below 10 K, at which point a small drop can be observed that indicates magnetically isotropic behaviour (Figure 6). Variable-frequency, variable-temperature ac magnetic susceptibility measurements were carried out to assess the magnetisation dynamics of **2** and **8**. However, neither of the compounds displayed peaks in the out-of-phase susceptibility (χ_M''), which indicates an absence of slow relaxation of magnetisation (Figures S22 and S23 in the Supporting Information).

Ab initio ligand field theory was employed to gain insights into the electronic structure of the full $[M^{I}\{N(SiMe_3)_2\}_2]^-$ (M = Cr, Mn,[14] Fe, Co) series. The computed splitting of the 3d orbitals exhibits a similar pattern for all complexes (Figure 7). In contrast to crystal field expectations for two-coordinate complexes, the lowest orbital is $3d_{z^2}$, which is stabilised by strong mixing with the 4s orbital. Along the Cr, Mn, Fe and Co series,

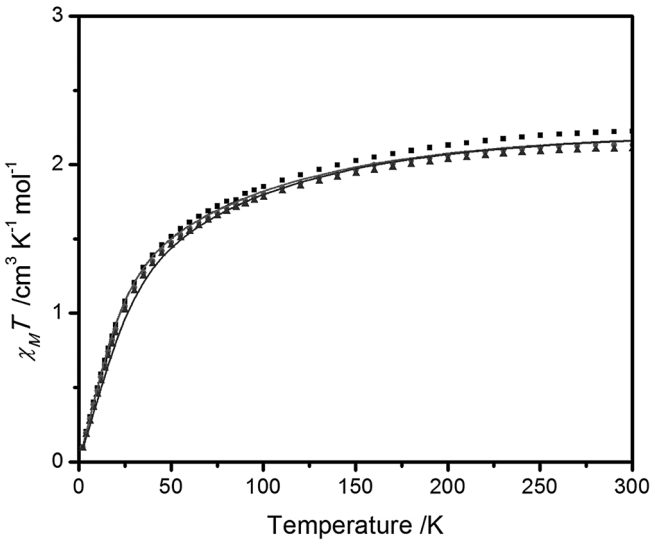

Figure 5. Variable-temperature molar magnetic susceptibility ($\chi_M T$) for **2**. Squares, circles, and triangles are data collected under applied dc fields of 0.1, 1, and 7 T, respectively. The data were fit simultaneously with PHI[28] to give the best fit, with $D = -100$ cm^{-1}, $|E/D| = 0.22$ cm^{-1}, $g_{\parallel} = 3.43$ and $g_{\perp} = 2.68$. The fits are shown as solid lines.

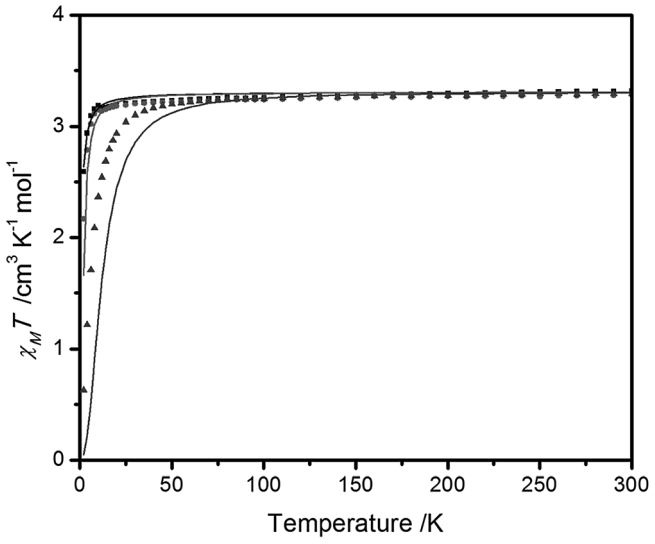

Figure 6. Variable-temperature molar magnetic susceptibility ($\chi_M T$) for **8**. Squares, triangles, and circles are data collected under applied dc fields of 0.1, 1, and 7 T, respectively. The data were fit simultaneously with PHI to give the best fit, with $D = 0.39$ cm^{-1}, $|E/D| = 5.5 \times 10^{-3}$ cm^{-1}, $g_{\parallel} = 2.43$ and $g_{\perp} = 1.91$. The fits are shown as solid lines.

the admixture of the 4s orbital into $3d_{z^2}$ decreases from 21 to 17, 14 and 11%, respectively, whereas the antibonding sigma interaction (e_{σ}) increases due to the shortening of the M–N bond (Table 1). Both effects bring the $3d_{z^2}$ orbital closer to the nearly degenerate, non-bonding d_{xy} and $d_{x^2-y^2}$ orbitals,[15] which experience only a small splitting caused by C_2 symmetry along the *z* axis. The d_{xz} and d_{yz} orbitals are split significantly (2200–2500 cm^{-1} for all complexes) due to a strong antibonding interaction between the nitrogen lone pair in the *yz* plane

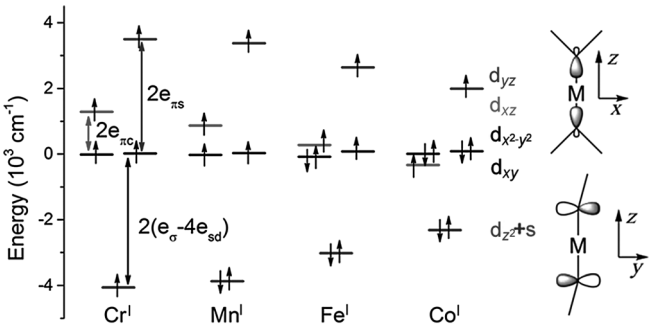

Figure 7. Structure and d-orbital splitting of $[M^I\{N(SiMe_3)_2\}_2]^-$, M = Cr (**3**), Mn (calculated), Fe (**1**), and Co (**2**).

with the d_{yz} orbital and a weak interaction between the N–Si bonding orbitals and the d_{xz} orbital. A stabilisation of the d_{xz} and d_{yz} orbitals is clearly observed along the series from Cr to Co due to enhanced π-bonding interactions at shorter M–N lengths. The ground-state electronic configuration shown in Figure 7 suggests orbitally non-degenerate ground states in the case of Cr^I and Mn^I and a doubly degenerate quartet ground state for Fe^I. In the case of Co^I, d_{xz} is lower than the d_{xy} and $d_{x^2-y^2}$ orbitals. Nevertheless, the dominant configuration in the ground-state wavefunction corresponds to singly occupied d_{xz} and d_{yz} orbitals.

The ground-state multiplet of each complex is split due to spin-orbit coupling with excited states. The corresponding zero-field splitting parameters *D* and *E/D* have been evaluated by using CASSCF/NEVPT2 with the effective spin-Hamiltonian formalism for the complexes with an orbitally non-degenerate ground state. The Cr^I complex has values of $D = 0.2$ cm^{-1} and $E/D = 0.3$ with an isotropic *g* tensor that is slightly smaller than the free electron value ($g_{iso} = 1.9999$), typical for $3d^5$ systems. The constructed Mn^I complex has a small zero-field splitting ($D = 1.9$ cm^{-1}, $E/D = 0.16$) and a nearly isotropic *g* tensor ($g_x \approx 2.00$, $g_y \approx 2.01$, $g_z \approx 2.02$). For Co^I, the estimated spin-Hamiltonian parameters show a pronounced anisotropy of the magnetic moment ($g_x = 2.06$, g_y 2.41, $g_z = 3.30$) and large but not ideally axial zero-field splitting ($D = -55$ cm^{-1} and $E/D = 0.16$).[16] Magnetic isotropy for Mn^I and non-axial anisotropy for Co^I explain the lack of observable slow relaxation of magnetisation.

The anion of **1** exhibits a degenerate ^{4}E ground-state splitting into four doublets, which are characterised best by the magnetic quantum number M_J (*J* = total angular moment). The four doublets would then correspond to $M_J = \pm 7/2$, $\pm 5/2$, $\pm 3/2$ and $\pm 1/2$, with an energy spacing between these doublets of approximately 210 cm^{-1}. The effective *g* tensor of the ground-state Kramers' doublet of $[Fe^I\{N(SiM_3)_2\}_2]^-$ has very pronounced axial anisotropy ($g_x = g_y = 0.0032$ and $g_z = 9.9851$). The calculated temperature dependence of magnetic susceptibility of **1** shows a maximum at approximately 150 K, characteristic for an orbitally degenerate ground state,[17] in accordance with the experimental results. These characteristics are very similar to those calculated for the related compound K(crypt.2.2.2)-$[Fe^I(C(SiMe_3)_3)_2]$.[2a] Nonetheless, the comparably lower experi-

mental barrier for **1** ($U_{eff}=48\ cm^{-1}$ vs. $U_{eff}=226\ cm^{-1}$ for $[Fe^{I}(C(SiMe_3)_3)_2]^-$) points to other relaxation mechanisms than over-barrier processes, which could result from vibrational distortion of the rather unencumbered amide ligand set.[18]

Conclusion

We have shown that anionic two-coordinate transition metal(I) complexes with $N(SiMe_3)_2^-$ ligands are stable structures not only for Fe (**1**),[7] but also for Cr and Co metal centres (**2**–**5**), which contrasts with Lewis base adducts or dimerisation processes observed for the +2 oxidation state with the same ligand set. In the case of Mn, very reactive dimeric complex **6** with an unsupported metal–metal bond was identified under the same reaction conditions. In this case, use of the bulkier $N(Dipp)SiMe_3^-$ ligand was necessary to stabilise a two-coordinate manganese(I) amide (**8**). Ab initio ligand field theory shed light on the electronic configuration and magnetic features of the $[M^{I}\{N(SiMe_3)_2\}_2]^-$ (M = Cr, Mn, Fe, Co) series. The study showed a similar orbital-splitting pattern along the series, with the most stable orbital being $3d_{z^2}$. Slow relaxation of magnetisation behaviour, observed only for the iron(I) complex, is explained by a calculated strong axial anisotropy.

Experimental Section

General

All manipulations were carried out in a glovebox or by using Schlenk-type techniques under a dry atmosphere of argon. Solvents were dried by using a MBraun solvent purification system and stored over KC_8. For details concerning the synthesis of starting materials, data acquisition of solution and solid-state analyses (^1H NMR, UV/Vis and IR spectroscopies, X-ray diffraction analysis, cyclovoltametry, magnetic measurements) and experimental spectra and solid state structures from X-Ray diffraction analysis, see the Supporting Information.

Synthesis of Complexes 2, 3, 5–8

K(18-crown-6)[Co{N(SiMe$_3$)$_2$}$_2$] (2)

$[Co\{N(SiMe_3)_2\}_2]\cdot(THF)_2$ (226 mg, 0.50 mmol) and 18-crown-6 (132 mg, 0.50 mmol) were dissolved in Et_2O (10 mL). Addition of KC_8 (93 mg, 0.75 mmol) resulted in an immediate colour change to greenish yellow. After stirring for 5 min, the mixture was filtered, the residue was extracted with Et_2O (2 mL) and the combined filtrates were layered with pentane (20 mL). Storing the solution at −37 °C for several days resulted in light green crystalline solids. Removal of the solvent by filtration, washing of the residue with pentane (2×5 mL) and drying afforded **2** as a pale-green crystalline solid (281 mg, 0.41 mmol, 82%). ^1H NMR ([D8]THF, 500.3 MHz, 298 K): $\delta=3.80$ (s, 24H, $w_{1/2}=4$ Hz, OCH_2), −4.70 ppm (s, 36H, $w_{1/2}=16$ Hz, $Si(CH_3)_3$); IR (ATR): $\tilde{\nu}=2941$ (w), 2893 (m), 1351 (w), 1233 (m), 1103 (vs), 988 (vs), 961 (s), 866 (m), 820 (vs), 660 (m), 609 cm^{-1} (w); elemental analysis calcd (%) for $C_{24}H_{60}CoKN_2O_6Si_4$ (683.12 $g\,mol^{-1}$): C 42.20, H 8.85, N 4.10; found: C 41.75, H 8.77, N 3.70; $\mu_{eff}=4.18\ \mu_B$ (Evans, [D8]THF + 1% TMS, 400.1 MHz, 298 K), $\mu_{S.O.}=2.83\ \mu_B$. Crystals suitable for X-ray diffraction analysis were obtained from a pentane-layered solution of **2** in Et_2O at −38 °C.

K(18-crown-6)[Cr{N(SiMe$_3$)$_2$}$_2$] (3)

$[Cr\{N(SiMe_3)_2\}_2]\cdot(THF)_2$ (259 mg, 0.53 mmol) and 18-crown-6 (132 mg, 0.50 mmol) were dissolved in Et_2O (15 mL). Addition of KC_8 (70 mg, 0.50 mmol) at 0 °C resulted in an immediate colour change to orange-yellow. After stirring the mixture for 10 min, the mixture was filtered and the residue extracted with Et_2O (2 mL). The solvents were removed under vacuum for several hours. The orange residue was extracted with Et_2O (5 mL) and the resulting filtrate was layered with pentane (15 mL) and stored at −37 °C for several days to give an orange-yellow crystalline solid. Removal of the solvent by filtration, washing of the residue with pentane (2× 5 mL) and drying of the crystalline residue afforded **3** (250 mg, 0.37 mmol, 71%). ^1H NMR ([D8]THF, 500.3 MHz, 298 K): $\delta=28.6$ ($w_{1/2}=500$ Hz, $Si(CH_3)_3$), 3.10 ppm ($w_{1/2}=124$ Hz, OCH_2); IR (ATR): $\nu=2936$ (m), 2896 (m), 1471 (vw), 1453 (vw), 1350 (w), 1283 (vw), 1230 (s), 1103 (vs), 1035 (s), 993 (m), 962 (s), 862 (m), 814 (vs), 761 (m), 657 (s), 606 (m), 530 (w), 412 cm^{-1} (w); elemental analysis calcd (%) for $C_{24}H_{60}CrKN_2O_6Si_4$ (675.19 $g\,mol^{-1}$): C 42.63, H 8.94, N 4.14; found: C 42.29, H 9.41, N 4.16; $\mu_{eff}=5.99\ \mu_B$ (Evans, [D8]THF + 1% TMS, 500.3 MHz, 298 K), $\mu_{S.O.}=5.91\ \mu_B$. Crystals suitable for X-ray diffraction analysis were obtained by storing a pentane-layered solution of **3** in Et_2O at −38 °C. Crystals of $(K(18\text{-crown-}6)_{1.5})[Cr\{N(SiMe_3)_2\}_2]$ (**4**) were observed in small quantities and characterised by using X-ray diffraction analysis (for the structure, see Figure S26 in the Supporting Information).

K(crypt.222)[Cr{N(SiMe$_3$)$_2$}$_2$] (5)

$[Cr\{N(SiMe_3)_2\}_2]\cdot(THF)_2$ (78 mg, 0.15 mmol) and crypt.222 (57 mg, 0.15 mmol) were dissolved in 5 mL of Et_2O. Addition of KC_8 (23 mg, 0.17 mmol) at 0 °C led to an immediate colour change from bright blue to orange yellow. After stirring the mixture for 5 min, the mixture was filtered, the residue was extracted with 2 mL of Et_2O and the combined filtrates were layered with pentane (10 mL) and stored at −37 °C for several days to give an orange-yellow crystalline solid. Filtration and washing of the residue with pentane (2× 5 mL) afforded **5** after drying under vacuum (110 mg, 0.12 mmol, 78%). ^1H NMR ([D8]THF, 400.1 MHz, 298 K): $\delta=28.2$ ($w_{1/2}=520$ Hz, $Si(CH_3)_3$), 3.43 ($w_{1/2}=40$ Hz, crypt.222), 2.53 ($w_{1/2}=28$ Hz, crypt.222), 0.73 ppm ($w_{1/2}=19$ Hz, crypt.222); IR (ATR): $\nu=2939$ (m), 2881 (m), 2814 (w), 1477 (vw), 1444 (vw), 1353 (m), 1283 (vw), 1230 (s), 1103 (s), 1077 (m), 997 (s), 950 (s), 931 (m), 863 (m), 815 (vs), 773 (s), 747 (m), 657 (s), 607 (m), 564 (w), 523 cm^{-1} (w); elemental analysis calcd (%) for $C_{30}H_{72}CrKN_4O_6Si_4$ (788.36 $g\,mol^{-1}$): C 45.71, H 9.21, N 7.11; found: C 45.56, H 9.85, N 6.96. Crystals suitable for X-ray diffraction analysis were obtained directly from the synthetic procedure.

Reduction of $[Mn\{N(SiMe_3)_2\}_2]_2$

$[K(18\text{-crown-}6)_{1.5}Mn\{N(SiMe_3)_2\}_2]_2$ (6) and decomposition products

A Pasteur pipette with KC_8 (20 mg, 0.15 mmol) on a filter plug was prepared and precooled to −38 °C. $[Mn\{N(SiMe_3)_2\}_2]$ (38 mg, 0.10 mmol) and 18-crown-6 (27 mg, 0.10 mmol) were dissolved in Et_2O (2 mL), cooled to −38 °C and added to the Pasteur pipette. Within ≈1 min, the colour changed to dark violet in the pipette. The solution was then filtered, layered with pentane (3 mL) and stored at −38 °C. Within 1–2 d, the formation of a red-violet solid can be observed, which was identified as $[\{K(18\text{-crown-}6)\}_2(\mu\text{-}18\text{-crown-}6)][(M\{N(SiMe_3)_2\}_2]_2$ (**6**) by using X-ray diffraction analysis. NMR spectroscopic data were obtained by performing the reduc-

tion in [D8]THF and immediately measuring the filtered solution. ^{1}H NMR ([D8]THF, 500.3 MHz, 298 K): $\delta = 3.94$ ($w_{1/2} = 53$ Hz, OCH_2), -10.94 ppm ($w_{1/2} = 500$ Hz, Si(CH_3)$_3$). Dissolution of the obtained crystals readily gave a discoloured solution that indicated decomposition. During the crystallisation process or on prolonged standing, a discolouration of the solution could be observed in addition to the formation of colourless crystals and an amorphous, dark brownish solid. X-ray diffraction analysis revealed that the crystals were K(18-crown-6)N(SiMe$_3$) and K(18-crown-6)[Mn{N(SiMe$_3$)$_2$}$_3$]. Yields could not be determined.

[Mn{N(Dipp)(SiMe$_3$)}$_2$](7)

Li{N(Dipp)(SiMe$_3$)} (980 mg, 3.84 mmol) was added to a suspension of anhydrous MnCl$_2$ (240 mg, 1.90 mmol) in Et$_2$O (30 mL). After stirring overnight at RT, all volatiles were removed under vacuum and the resulting residue extracted with pentane (3×10 mL). The combined filtrates were concentrated and stored at $-37\,^\circ$C. After several days, yellow crystals of **7** were isolated (600 mg, 1.09 mmol, 57%). Complex **7** shows no signal in the ^{1}H NMR spectrum; IR (ATR): $\tilde{\nu} = 2959$ (m), 2867 (w), 1456 (w), 1422 (s), 1310 (m), 1238 (s), 1188 (s), 1108 (m), 1038 (m), 916 (vs), 878 (m), 828 (vs), 785 (vs), 744 (s) 669 (s), 628 (w), 532 (m), 419 cm^{-1} (m); elemental analysis calcd (%) for C$_{30}$H$_{52}$MnN$_2$Si$_2$ (551.58 g mol^{-1}): C 65.29, H 9.50, N 5.08; found: C 65.32, H 10.25, N 5.07. No matching H value could be obtained even when using crushed, freshly prepared crystals; an approx. 1% higher value was always observed (>5 tries); $\mu_{eff} = 6.02\ \mu_B$ (Evans, C$_6$D$_6$ + 1% TMS, 400.1 MHz, 298 K), $\mu_{S.O.} = 5.91\ \mu_B$. Crystals suitable for X-ray diffraction analysis were obtained directly from the synthetic procedure.

K(18-crown-6)[Mn{N(Dipp)SiMe$_3$}$_2$] (8)

Complex **7** (275 mg, 0.50 mmol) was dissolved in Et$_2$O (10 mL) and KC$_8$ (80 mg, 0.55 mmol) were added. After stirring for 5 min, the resulting dark-violet solution was filtered and layered with 18-crown-6 (140 mg, 0.50 mmol) in Et$_2$O (25 mL), then stored at $-37\,^\circ$C to give a dark-violet crystalline solid. After removal of the solution by filtration, and washing the residue with pentane (5 mL), the resulting violet solid was dried under vacuum to give complex **8** (260 mg, 0.30 mmol, 60%). ^{1}H NMR ([D8]THF, 500.3 MHz, 298 K): $\delta = 15.3$ ($w_{1/2} = 1200$ Hz), 11.0 ($w_{1/2} = 200$ Hz); 3.85 ($w_{1/2} = 50$ Hz, OCH_2), 0.3 ($w_{1/2} = 130$ Hz), -12.4 ppm ($w_{1/2} = 500$ Hz); IR (ATR): $\tilde{\nu} =$ 2948 (m), 2911 (w), 2890 (m), 2859 (m), 1452 (w), 1419 (m), 1374 (vw), 1350 (m), 1314 (m), 1239 (s), 1228 (m), 1196 (m), 1101 (vs), 1051 (w), 1039 (w), 961 (s), 932 (s), 828 (vs), 779 (s), 740 (m), 661 (m), 618 (w), 531 (m), 424 cm^{-1} (m); elemental analysis calcd (%) for C$_{42}$H$_{76}$KMnN$_2$O$_6$Si$_2$ (855.28 g mol^{-1}): C 58.98, H 8.96, N 3.28; found: C 58.59, H 9.40, N 3.15; $\mu_{eff} = 4.98\ \mu_B$ (Evans, [D8]THF + 1% TMS, 400.1 MHz, 298 K), $\mu_{S.O.} = 4.89\ \mu_B$. Crystals suitable for X-ray diffraction analysis were obtained directly from the synthetic procedure.

Quantum Chemical Calculations

The ORCA quantum chemistry program was used for all calculations.[19,20] The ground and excited states of corresponding d^n configurations were computed by using the state-averaged complete active space self-consistent field (SA-CASSCF)[21] method with the relativistically contracted version[22] of the def2-TZVP basis set.[23] The scalar relativistic effects were taken into account by using the standard second-order Douglas–Kroll–Hess procedure.[24] The resolution of identity approximation was employed to speed up the calculations.[25] The additional N-electron valence perturbation theory to second-order (NEVPT2)[26] energy correction has been done. The energies and wavefunctions of all magnetic sublevels were computed by diagonalisation of the full SOC matrix. The spin-Hamiltonian parameters were evaluated by using the effective Hamiltonian approach.[27]

Crystallographic Data

CCDC 1414086 (**2**), 1414087 (**3**), 1414088 (**4**), 1414089 (**5**), 1414090 (**6**), 1414091 (**7**), 1414092 (**8**), 1415012 (**9**), and 1415011 (**10**) contain the supplementary crystallographic data for this paper. These data are provided free of charge by The Cambridge Crystallographic Data Centre.

Acknowledgements

C.G.W., S.B. and S.S.E. thank the ANR (programme blanc "IRONHYC" ANR-12), the DFG (WE 5627/1-1 personal grant for C.G.W.) and the CNRS for financial support. Collection and analysis of the magnetic susceptibility data were supported by NSF grant (CHE-1464841) to J.R.L.

Keywords: ab initio calculations · magnetic properties · N ligands · transition metals · coordination modes

[1] a) D. L. Kays, *Dalton Trans.* **2011**, *40*, 769–778; b) P. P. Power, *Chem. Rev.* **2012**, *112*, 3482–3507.

[2] For anionic two-coordinate metal(I) complexes, see: a) J. M. Zadrozny, D. J. Xiao, M. Atanasov, G. J. Long, F. Grandjean, F. Neese, J. R. Long, *Nat. Chem.* **2013**, *5*, 577–581; b) J. M. Zadrozny, D. J. Xiao, J. R. Long, M. Atanasov, F. Neese, F. Grandjean, G. J. Long, *Inorg. Chem.* **2013**, *52*, 13123–13131; c) M. I. Lipschutz, X. Yang, R. Chatterjee, T. D. Tilley, *J. Am. Chem. Soc.* **2013**, *135*, 15298–15301; d) I. C. Cai, M. I. Lipschutz, T. D. Tilley, *Chem. Commun.* **2014**, *50*, 13062–13065; e) C.-Y. Lin, J. C. Fettinger, F. Grandjean, G. J. Long, P. P. Power, *Inorg. Chem.* **2014**, *53*, 9400–9406; f) C. Y. Lin, J. C. Fettinger, N. F. Chilton, A. Formanuik, F. Grandjean, G. J. Long, P. P. Power, *Chem. Commun.* **2015**, *51*, 13275–13278.

[3] For neutral and cationic two-coordinate M^{I} complexes, see: a) R. Wolf, C. Ni, T. Nguyen, M. Brynda, G. J. Long, A. D. Sutton, R. C. Fischer, J. C. Fettinger, M. Hellman, L. Pu, P. P. Power, *Inorg. Chem.* **2007**, *46*, 11277–11290; b) C. A. Laskowski, G. L. Hillhouse, *J. Am. Chem. Soc.* **2008**, *130*, 13846–13847; c) Z. Mo, D. Chen, X. Leng, L. Deng, *Organometallics* **2012**, *31*, 7040–7043; d) C. A. Laskowski, D. J. Bungum, S. M. Baldwin, S. A. Del Ciello, V. M. Iluc, G. L. Hillhouse, *J. Am. Chem. Soc.* **2013**, *135*, 18272–18275; e) P. P. Samuel, K. C. Mondal, H. W. Roesky, M. Hermann, G. Frenking, S. Demeshko, F. Meyer, A. C. Stückl, J. H. Christian, N. S. Dalal, L. Ungur, L. F. Chibotaru, K. Pröpper, A. Meents, B. Dittrich, *Angew. Chem. Int. Ed.* **2013**, *52*, 11817–11821; *Angew. Chem.* **2013**, *125*, 12033–12037; f) G. Ung, J. Rittle, M. Soleilhavoup, G. Bertrand, J. C. Peters, *Angew. Chem. Int. Ed.* **2014**, *53*, 8427–8431; *Angew. Chem.* **2014**, *126*, 8567–8571; g) P. P. Samuel, K. C. Mondal, N. Amin Sk, H. W. Roesky, E. Carl, R. Neufeld, D. Stalke, S. Demeshko, F. Meyer, L. Ungur, L. F. Chibotaru, J. Christian, V. Ramachandran, J. van Tol, N. S. Dalal, *J. Am. Chem. Soc.* **2014**, *136*, 11964–11971; h) Z. Mo, Z. Ouyang, L. Wang, K. L. Fillman, M. L. Neidig, L. Deng, *Org. Chem. Front.* **2014**, *1*, 1040–1044; i) P. P. Samuel, R. Neufeld, K. Chandra Mondal, H. W. Roesky, R. Herbst-Irmer, D. Stalke, S. Demeshko, F. Meyer, V. C. Rojisha, S. De, P. Parameswaran, A. C. Stuckl, W. Kaim, J. H. Christian, J. K. Bindra, N. S. Dalal, *Chem. Sci.* **2015**, *6*, 3148–3153; j) J. Hicks, C. Jones, *Organometallics* **2015**, *34*, 2118–2121.

[4] For bimetallic Mn^{I} complexes featuring a metal–metal bond, see: J. Hicks, C. E. Hoyer, B. Moubaraki, G. L. Manni, E. Carter, D. M. Murphy, K. S. Murray, L. Gagliardi, C. Jones, *J. Am. Chem. Soc.* **2014**, *136*, 5283–5286.

[5] E. Sheng, S. Wang, G. Yang, S. Zhou, L. Cheng, K. Zhang, Z. Huang, *Organometallics* **2003**, *22*, 684 – 692.
[6] a) R. E. Mulvey, S. D. Robertson, *Angew. Chem. Int. Ed.* **2013**, *52*, 11470 – 11487; *Angew. Chem.* **2013**, *125*, 11682 – 11700; b) M. P. Coles, *Coord. Chem. Rev.* **2015**, *297 – 298*, 2 – 23.
[7] C. G. Werncke, P. C. Bunting, C. Duhayon, J. R. Long, S. Bontemps, S. Sabo-Etienne, *Angew. Chem. Int. Ed.* **2015**, *54*, 245 – 248; *Angew. Chem.* **2015**, *127*, 247 – 250.
[8] Using the more encapsulating cryptand crypt.2.2.2 or lowering the temperature of reduction to −110 °C proved unfruitful. Notable reduction only occurs at temperatures higher than ≈ −20 °C.
[9] a) J. Chai, H. Zhu, A. C. Stückl, H. W. Roesky, J. Magull, A. Bencini, A. Caneschi, D. Gatteschi, *J. Am. Chem. Soc.* **2005**, *127*, 9201 – 9206; b) D.-Y. Lu, J.-S. K. Yu, T.-S. Kuo, G.-H. Lee, Y. Wang, Y.-C. Tsai, *Angew. Chem. Int. Ed.* **2011**, *50*, 7611 – 7615; *Angew. Chem.* **2011**, *123*, 7753 – 7757.
[10] B. D. Murray, P. P. Power, *J. Am. Chem. Soc.* **1984**, *106*, 7011 – 7015.
[11] a) S. Pfirrmann, S. Yao, B. Ziemer, R. Stösser, M. Driess, C. Limberg, *Organometallics* **2009**, *28*, 6855 – 6860; b) W. H. Monillas, G. P. A. Yap, L. A. MacAdams, K. H. Theopold, *J. Am. Chem. Soc.* **2007**, *129*, 8090 – 8091; c) J. M. Smith, A. R. Sadique, T. R. Cundari, K. R. Rodgers, G. Lukat-Rodgers, R. J. Lachicotte, C. J. Flaschenriem, J. Vela, P. L. Holland, *J. Am. Chem. Soc.* **2006**, *128*, 756 – 769.
[12] Only the trigonal THF adduct has been reported, see: D. K. Kennepohl, S. Brooker, G. M. Sheldrick, H. W. Roesky, *Z. Naturforsch. B: Chem. Sci.* **1992**, *47*, 9 – 16.
[13] C.-Y. Lin, J.-D. Guo, J. C. Fettinger, S. Nagase, F. Grandjean, G. J. Long, N. F. Chilton, P. P. Power, *Inorg. Chem.* **2013**, *52*, 13584 – 13593.
[14] The $[Mn^{I}\{N(SiMe_3)_2\}_2]^-$ complex was calculated based on **1** with Mn–N bonds adjusted to 1.961 Å, as found in **8**.
[15] The barycentre of d_{xy} and $d_{x^2-y^2}$ is set to zero.
[16] Due to low-lying excited states of the Co^{I} complex ($<1000\ cm^{-1}$, see the Supporting Information for details), the spin-Hamiltonian formalism approximation might be questioned and one can expect a large TIP (temperature independent behaviour) contribution to magnetic susceptibility.
[17] M. Kotani, *J. Phys. Soc. Jpn.* **1949**, *4*, 293 – 297.
[18] M. Atanasov, J. M. Zadrozny, J. R. Long, F. Neese, *Chem. Sci.* **2013**, *4*, 139 – 156.
[19] F. Neese, *Wires Comput. Mol. Sci.* **2012**, *2*, 73 – 78.
[20] F. Neese, with contributions from U. Becker, G. Ganyushin, A. Hansen, R. Izsak, D. G. Liakos, C. Kollmar, S. Kossmann, D. A. Pantazis, T. Petrenko, C. Reimann, C. Riplinger, M. Roemelt, B. Sandhöfer, I. Schapiro, K. Sivalingam, F. Wennmohs, B. Wezisla and contributions from our collaborators: M. Kállay, S. Grimme, E. Valeev, ORCA - An ab initio, DFT and semi-empirical SCF-MO package, Version 3.0; Mülheim a. d. R. The binaries of ORCA are available free of charge for academic users for a variety of platforms.
[21] a) B. O. Roos, P. R. Taylor, P. E. M. Siegbahn, *Chem. Phys.* **1980**, *48*, 157 – 173; b) P. Siegbahn, A. Heiberg, B. Roos, B. Levy, *Phys. Scripta* **1980**, *21*, 323 – 327; c) P. E. M. Siegbahn, J. Almlof, A. Heiberg, B. O. Roos, *J. Chem. Phys.* **1981**, *74*, 2384 – 2396.
[22] D. A. Pantazis, X. Y. Chen, C. R. Landis, F. Neese, *J. Chem. Theory Comput.* **2008**, *4*, 908 – 919.
[23] a) A. Schäfer, C. Huber, R. Ahlrichs, *J. Chem. Phys.* **1994**, *100*, 5829 – 5835; b) F. Weigend, R. Ahlrichs, *Phys. Chem. Chem. Phys.* **2005**, *7*, 3297 – 3305; c) A. Schäfer, H. Horn, R. Ahlrichs, *J. Chem. Phys.* **1992**, *97*, 2571 – 2577.
[24] B. A. Hess, *Phys. Rev. A* **1986**, *33*, 3742 – 3748.
[25] F. Neese, *J. Comput. Chem.* **2003**, *24*, 1740 – 1747.
[26] a) C. Angeli, R. Cimiraglia, J.-P. Malrieu, *Chem. Phys. Lett.* **2001**, *350*, 297 – 305; b) C. Angeli, R. Cimiraglia, J.-P. Malrieu, *J. Chem. Phys.* **2002**, *117*, 9138 – 9153; c) C. Angeli, R. Cimiraglia, S. Evangelisti, T. Leininger, J.-P. Malrieu, *J. Chem. Phys.* **2001**, *114*, 10252 – 10264; d) C. Angeli, R. Cimiraglia, *Theor. Chem. Acc.* **2002**, *107*, 313 – 317.
[27] V. Vallet, L. Maron, C. Teichteil, J.-P. Flament, *J. Chem. Phys.* **2000**, *113*, 1391 – 1402.
[28] N. F. Chilton, R. P. Anderson, L. D. Turner, A. Soncini, K. S. Murray, *J. Comput. Chem.* **2013**, *34*, 1164 – 1175.

Received: October 5, 2015
Published online on ■■ ▮▮, 0000

FULL PAPER

Transition Metals

C. G. Werncke, E. Suturina, P. C. Bunting, L. Vendier, J. R. Long, M. Atanasov, F. Neese, S. Sabo-Etienne, S. Bontemps**

■■ – ■■

Homoleptic Two-Coordinate Silylamido Complexes of Chromium(I), Manganese(I), and Cobalt(I)

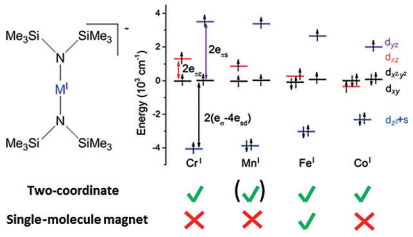

Amido magnetism: The amido $N(SiMe_3)_2^-$ ligand is shown to stabilise two-coordinate metal(I) complexes for Cr and Co, in a manner similar to that previously reported for the Fe analogue (see figure). In the case of Mn, a dimer with an unsupported Mn–Mn bond was isolated. Quantum chemical calculation provided an electronic and magnetic description of the Cr–Co series.